Citrate-dependent Heparan Sulfate-mediated Cell Surface Retention of Cobra Cardiotoxin A3

Anionic citrate is a major component of venom, but the role of venom citrate in toxicity is poorly understood other than inhibitory effect on the cation-dependent action of venom toxins. X-ray determination of CTX A3-heparin hexasaccharide complex structure reveals a molecular mechanism of citrate-induced dimerization of CTXs by interacting with Lys31 near the tip of loop 2 to stabilize the hydrophobic contact of the dimeric CTX A3 at the functionally important loop 1 and loop 2 regions. Our result suggests a novel role for venom citrate activity and identify specific sulfation pattern of HS in binding to CTX A3 for exerting cytotoxicity. It also reveals a structural model on how HS-CTX interaction could stabilize the CTX-lipid membrane interaction.

Citrate is present as a major component of snake, bee, scorpion and ant venom and serves as counter ion for the basic polypeptides of many venoms. For instance, ~ 50 mM citrate is present in Taiwan cobra (*Naja atra*) venom. The role of citrate as a divalent cationic chelator that inhibits calcium ion dependent enzyme activity in venom storage glands has been established. The function of citrate in the envenomed host, however, remains elusive. Interestingly, citrate serves as a buffer component and often mediates a monomer-dimer equilibrium of many proteases for regulation of their catalytic activity by either stabilizing the active dimeric form or, indirectly, the protease oxyanion hole. Citrate has been used in many protein crystallization studies and has been observed to be located at functionally important anionic binding pockets. For instance, co-crystallization of citrate with the membrane phosphatidylinositol 3-phosphate (PIP) binding protein of Hrs has been shown to directly promote PIP dimerization through two FYVE tandem domains. It suggests a structural model of PIP/Hrs based on citrate binding conformation.

Cell surface retention of biologically active ligands through heparin or heparan sulfate (HS) binding plays an important role not only in certain disease states but also in cell development. Heparin and HS are a class of glycosaminoglycans (GAGs) that are widely distributed in many tissues and cell types. They are negatively charged polymers composed of heterogeneous disaccharide repeating units of uronate-glucosamine (IdoA/GlcA-α1-4-GlcN). An uneven sulfation pattern, especially *N*-substitution differences, accounts for heterogeneity and provides the structural basis for the specific binding of extracellular regulatory proteins to exert their biological functions. Glycosaminoglycans have also been suggested to play biological roles as regulators of the transport and effector functions of numerous extracellular regulatory proteins, including growth factors, proteases, lipoprotein lipase, che-mokines, morphogens and viral proteins.

Cobra cardiotoxins (CTXs) are basic proteins with different GAG-binding specificities conferred by a cationic belt of the conserved residues and the availability of specific Lys residues. They constitute ~ 50 % of the venom by weight and are composed of 60-62 amino acids, with β-sheets forming three fingered loop structures (Table 1). Interestingly, heparin binding not only stabilizes the membrane-bound form of CTXs, but also induces CTX aggregation. Subcutaneous injection of cobra toxin in mice suggested that certain CTXs, unlike other venom components, remained at the sites of lesion

***Table 1:** Comparison in primary sequence of CTX homologuses.*

CTX	10	20	30	40	50	60
atra A3	LKC NKLVPLF YKTCPAGKNL CYKMFMVATP KVPVKRGCID VCPKSSLLVK YVCCNTDRCN					
atra A4b	LKC NKLVPLF YKTCPAGKNL CYKMFMVSNK MVPVKRGCID VCPKSSLLVK YVCCNTDRCN					
atra A5	LKCHNTQLPFI YKTCPEGKNL CFKATLKKFPLKFPVKRGCAD NCPKNSALLK YVCCSTDKCN					
atra A6	LKC NQLIPPF YKTCAAGKNL CYKMFMVAAP KVPVKRGCID VCPKSSLLVK YVCCNTDRCN					
mossambica M4	LKC NRLIPPF WKTCPEGKNL CYKMTMRLAP KVPVKRGCID VCPKSSLLIK YMCCNTNKCN					
mossambica M2	LKC NQLIPPF WKTCPKGKNL CYKMTMRGAS KVPVKRGCID VCPKSSLLIK YMCCNTDKCN					
mossambica M3	LKC NKLIPIA YKTCPEGKNL CYKMMLASKK MVPVKRGCIN VCPKNSALVK YVCCSTDRCN					
kaouthia Cytotoxin II	LKC NKLIPLA YKTCPAGKNL CYKMFMVAAP KVPVKRGCID ACPKNSLLVK YVCCNTDRCN					
kaouthia CLBP	LKCHNTQLPFI YKTCPEGKNL CFKATLKKFPLKIPIKRGCAD NCPKNSALLK YVCCSTDKCN					
kaouthia CM-7a	LKC NKLIPLA YKTCPAGKNL CYKMFMVSNK TVPVKRGCID VCPKNSLLVK YVCCNTDRCN					
kaouthia CM-7	LKC NKLIPLA YKTCPAGKNL CYKMFMVSNK TVPVKRGCID ACPKNSLLVK YVCCNTDRCN					
naja Cobramine A	LKC NKLIPLA YKTCPAGKNL CYKMYMVSNK TVPVKRGCID VCPKNSLVLK YECCNTDRCN					
naja Cobramine B	LKC NKLVPLF YKTCPAGKNL CYKMYMVATP KVPVKRGCID VCPKSSLVLK YVCCNTDRCN					
naja CLBP	LKCHNTQLPFI YKTCPEGKNL CFKATLKKFPLKFPVKRGCAD NCPKNSALLK YVCCSTDKCN					
nigricollis Tγ	LKC NQLIPPF WKTCPKGKNL CYKMTMRAAP MVPVKRGCID VCPKSSLLIK YMCCNTDKCN					
atra A1	LKC NKLIPIA SKTCPAGKNL CYKMFMMSDL TIPVKRGCID VCPKNSLLVK YVCCNTDRCN					
atra A2	LKC NKLVPLF YKTCPAGKNL CYKMFMVSNL TVPVKRGCID VCPKNSALVK YVCCNTDRCN					
atra A4	RKC NKLVPLF YKTCPAGKNL CYKMFMVSNL TVPVKRGCID VCPKNSALVK YVCCNTDRCN					
mossambica M1	LKC NQLIPPF WKTCPKGKNL CYKMTMRAAP MVPVKRGCID VCPKSSLLIK YMCCNTNKCN					
haje CM-7	LKC HQLVPPF WKTCPEGKNL CYKMYMVATP MIPVKRGCID VCPKNSALVK YMCCNTDKCN					
haje CM-8	LKC HQLVPPF WKTCPEGKNL CYKMYMVSSS TVPVKRGCID VCPKNSALVK YVCCNTDKCN					
haje CM-9	LKC HQLVPPF WKTCPAGKNL CYKMYMVATP MIPVKRGCID VCPKNSALVK YMCCNTDKCN					
haje CM-10b	LKC HKLVPPF WKTCPEGKNL CYKMYMVATP MIPVKRGCID VCPKNSALVK YVCCNTDKCN					
kaouthia CM-6	LKC NKLIPIA SKTCPAGKNL CYKMFMMSDL TIPVKRGCID VCPKNSLLVK YVCCNTDRCN					

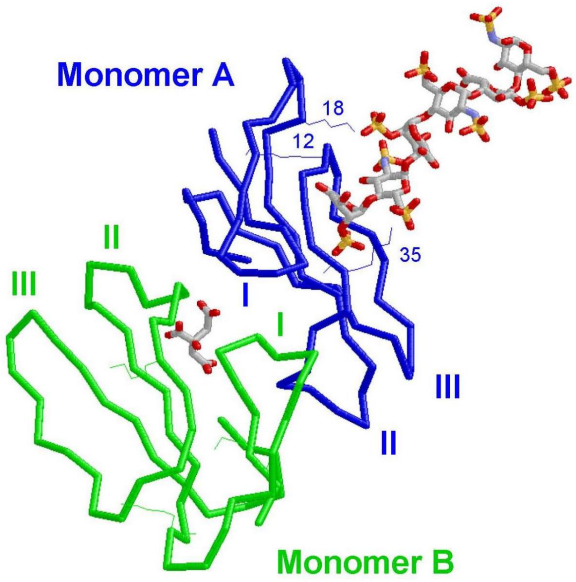

Fig. 1: Dimeric packing of CTX A3 with one heparin hexasaccharide bound to the positively charged cluster composed of Lys12, Lys18, and Lys35 in monomer A (blue). The two CTX A3 molecules are shown in as the alpha carbon backbone while the heparin hexasaccharide and citrate are shown in stick representations.

by unknown molecular mechanisms. Considering that various homologous CTXs from the venoms of *naja atra* and other cobras, *naja nigricollis* and *naja mossambica*, have diverse potential biological targets in a wide range of cell membranes, it is of interest to investigate whether the interaction of GAGs with CTXs plays a role in mediating tissue retention of specific CTX types and whether other venom components are also involved in retention.

In order to understand the action mechanism of citrate-dependent heparin-mediated cell retention, CTX A3 was co-crystallized with fully-sulfated heparin hexasaccharide in the presence of citrate ions and the structure of CTX A3 in complex with hexasaccharide was determined at 2.4 Å resolution. As shown in Fig. 1, there are two CTX A3 molecules with pseudo 2-fold symmetry, one citrate and one heparin hexasaccharide per asymmetric unit. The crystal structure of CTX A3 shows the general three-fingered CTX folding and contains five β-sheets comprising residues 2-4 (β1), 11-13 (β2), 20-26 (β3), 35-39 (β4) and 49-54 (β5). Three functional loops are formed by residues 4-11 (loop I), 26-35 (loop II) and 39-49 (loop III) (Fig. 1). Dimer formation buried approximately 1100 $Å^2$ of accessible surface area of the two monomers with approximately 300 $Å^2$ of polar and 800 $Å^2$ of non-polar contact areas. The major contacts of the dimer are from the hydrophobic residues at both the loop I and loop II regions, namely, Leu6, Val7, Pro8, Leu9 of loop I and Val32 and Pro33 of loop II.

One citrate ion (an essential component in the crystallization buffer which contained 0.1 M sodium citrate) resided at the interface of two monomers near Lys31 and Lys23 of monomers A and B (Fig. 2). The citrate ion occupied a strongly cationic pocket generated by CTX A3 dimerization (Fig. 3). Both Lys23 and Lys31 stabilized the citrate ion with electrostatic interaction distances of approximately 3 Å. Although Lys-23 is conserved through all the CTX homologues (Table 1), CTXs can be classified into two groups based simply on the presence and absence of Lys-31 near the tip of loop II.

Two positively charged clusters on the CTX A3 dimer (Fig. 3), identified previously by an NMR study of heparin disaccharide binding to CTX A3, constitute a potential long-chain heparin binding site (Fig. 1). However, the heparin hexasaccharide only makes contact with monomer A at the convex heparin-binding site in each unit cell (Fig. 1). The other ligand free positively charged cluster is located on the same side of the CTX A3 dimer at a distance of 25 Å -30 Å. Since our SPR studies use high molecular weight heparin (typically with average chain length of ~ 250 Å), a further extention of heparin chain length by 6-7 disaccharide repeats could help explain the observed citrate-dependent retention of CTX binding.

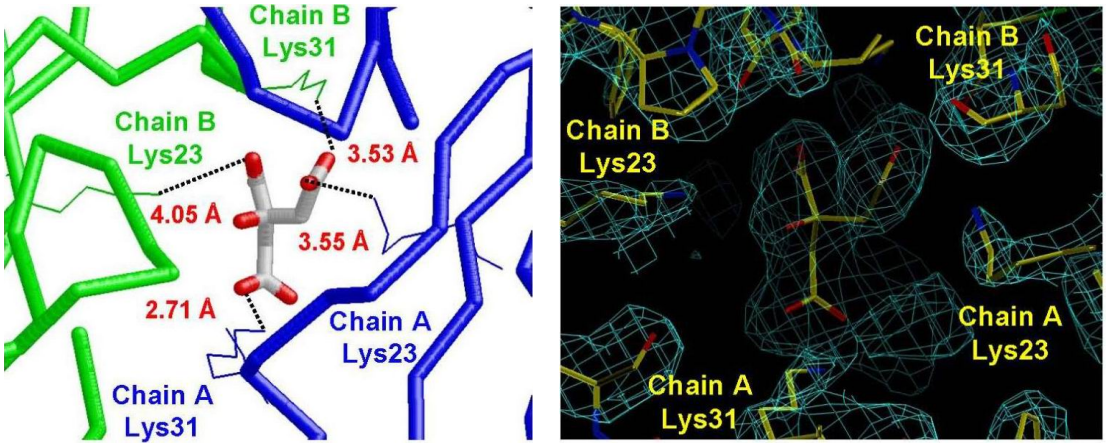

Fig. 2: Citrate bound to Lys31 and Lys23 of monomer A and B with an electrostatic contact of 3-4 Å. B (bottom), $2F_oFc$ electron density map for the citrate ion and the charged cluster formed by Lys31 and Lys23 of the two monomers.

Comparison of the two CTX A3 monomers shows an overall r.m.s. deviation of 1.17 Å over 60 residues. The most significant structural variations of the backbone main chains between the two monomers (monomer A with bound heparin and monomer B without bound heparin) occur at CTX core surrounding Cys14 and Cys38. In fact, a heparin-induced conformational change is observed for the Cys14-Cys38 disulfide bridge as reflected by the significant change (>30 degrees) of the disulfide bond torsion angles. Previously, by comparing the NOE intensity change in a ^{1}H NMR study of heparin-binding to the CTX A3, we showed that a significant heparin-induced conformational and/or dynamic change occurs near the Cys-38 core region. Our current X-ray structure further suggests that heparin-induced conformational change of CTX A3 at the core region indeed occurs perturbing the β-sheet structure.

In addition to the conformational change of the main chain, there are also several heparin-induced changes in side chain orientation as indicated in Fig. 4. Basically, two major types of structural perturbation are observed, one associated mainly with residues, such as Lys18, Lys44, Lys23, and Lys31, involved in electrostatic interaction with either heparin or citrate (Fig. 5) and the other associated with residues involved in hydrophobic side interactions such as Leu9 and Met26 located at the tips of loops I and II. Since both X-ray and NMR methods detect a similar heparin-induced conformational change in both the main chain and side chains, our results strongly suggest that the heparin-induced conformational change observed in the crystalline state may also occur in solution.

The electron density of fully sulfated hexasaccharide at 2.4 Å resolution (Fig. 5) is clear enough to allow us to determine its molecular orientation and atomic contacts relative to CTX A3 (Fig. 5). The heparin hexasaccharide binds to monomer A through the first three carbohydrate residues from the non-reducing end, which is consistent with the fact that reducing end of heparan sulfate is linked to core protein of proteoglycans. The overall crystal packing showed, however, additional hexasaccharide contacts, at both the reducing

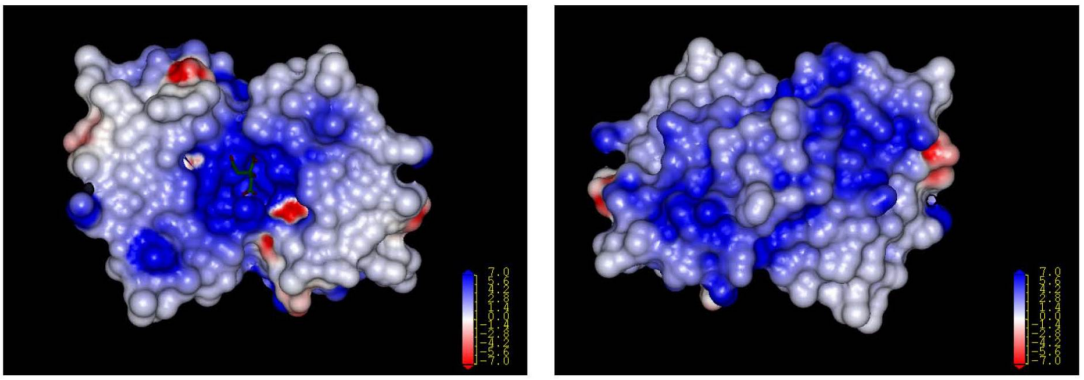

Fig. 3: Left, Electrostatic surface of the CTX A3 dimer showing citrate bound to a highly positively charged cluster generated by dimer formation. Right, View of CTX A3 dimer showing two heparin binding sites that are potential sites for toxin retention on heparin surfaces.

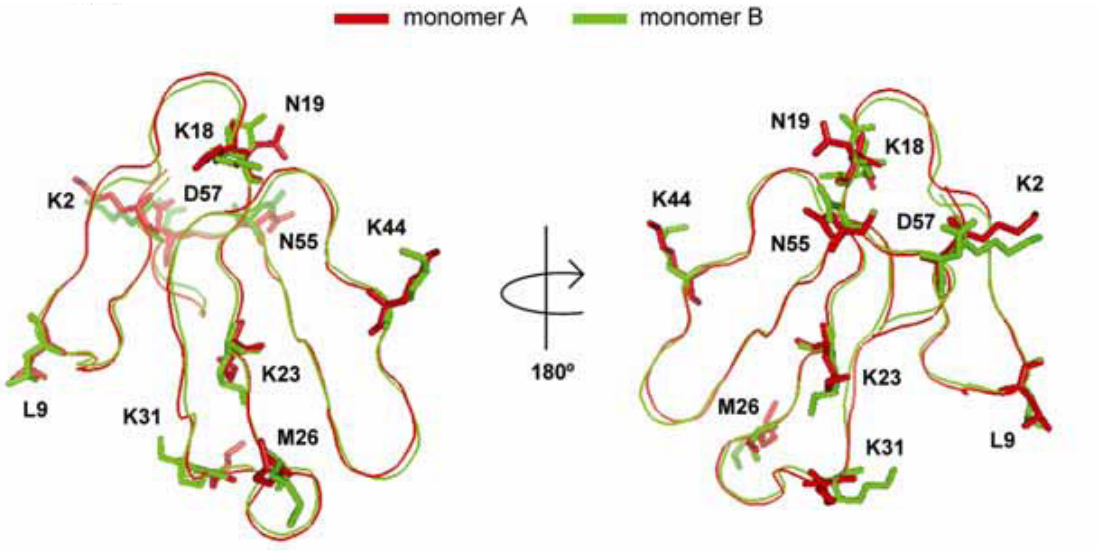

Fig. 4: Conformational changes induced in CTX A3 by heparin binding.

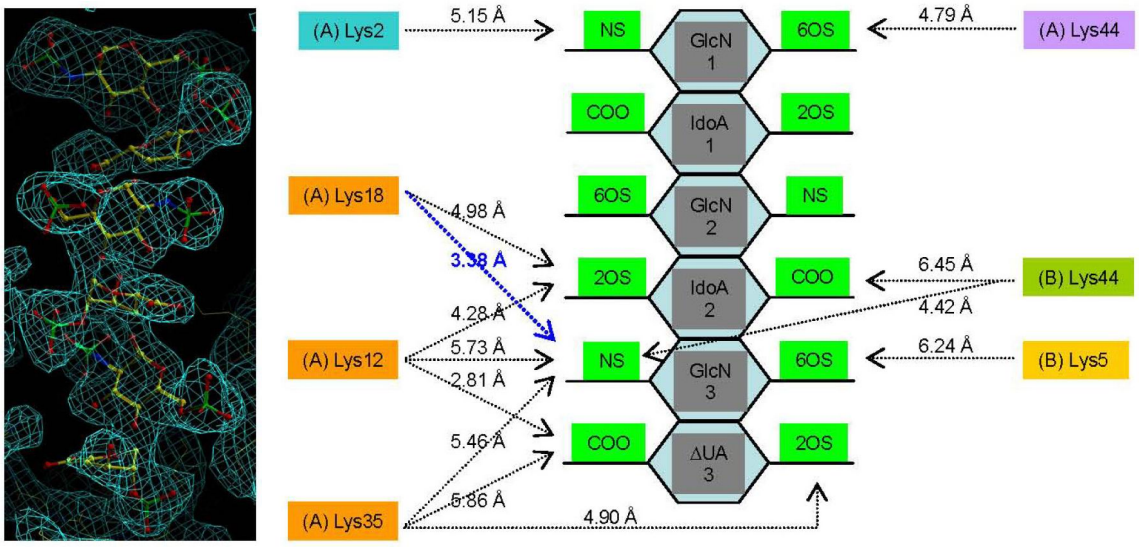

***Fig. 5**: Left, $2F_0Fc$ electron density map for heparin hexasaccharide. Right, Schematic diagram of interactions between CTX A3 and heparin hexasaccharide. The repeat units of glucosamine (GlcN), iduronic acid (IdoA) and unsaturated uronic acid (ΔUA) are assigned from the reducing end to the non-reducing end. The sulfation patterns are abbreviated as: NS, N-sulfate; 2OS, 2-O-sulfate; 6OS, 6-O-sulfate. Amino acid residues from different CTX monomers are shown in different colors.*

and non-reducing ends, with neighboring CTX A3 dimers (Fig. 5). The ring conformations of GlcN residues in heparin hexasaccharide are all $^4C_1$. The first and second IdoA are in the $^2S_0$ and $^1C_4$ conformation, respectively while the terminal uronate adapts a $^1H_2$ conformation. All the ring conformations fall into the predicted energy minima of conformational equilibria. The plot of torsional angles (Φ, Ψ) of the determined heparin conformation allows a further check of the obtained structure. By taking 26 available heparin coordinates from 14 PDB structures, we obtained the torsion angles for 55 GlcN-UA and 57 UA-GlcN linkages. The average of torsion angles (Φ, Ψ) with standard deviation found to be (83±20, 98±18) and (-73±13, 133±16) for GlcN-UA and UA-GlcN linkage, respectively. Our heparin bound conformation is therefore consistent with most conformations determined by either NMR or X-ray methods.

Close examination of electrostatic interactions showed the basis of the specificity of the heparin-CTXA3 interaction (Fig. 5). Of the sulfate groups, one *N*-sulfate (on GlcN3 as labeled in Fig. 5) interacted simultaneously with Lys18, Lys12, and Lys35 of monomer A and Lys44 of monomer B. The 2-*O*-sulfate groups were also important since three contacts existed for Lys18, Lys12, and Lys35 of monomer A. Only one interaction was observed for 6-*O*-sulfate with Lys5 of neighboring monomer B. The carboxylate groups also play an important role in CTXA3-heparin interaction as depicted in the figure.

BEAMLINE
17B2 W20 Protein Crystallography beamline
SP12B2 Protein X-ray Crystallography beamline

EXPERIMENTAL STATION
Protein Crystallography end station

AUTHORS
H.-S. Guan and C.-J. Chen
National Synchrotron Radiation Research Center, Hsinchu, Taiwan

S.-C. Lee, C.-H. Wang, W.-N. Huang, S.-C. Tjong, and W.-G. Wu
Institute of Bioinformatics and Structural Biology, National Tsing-Hua University, Hsinchu, Taiwan

PUBLICATIONS
- S.-C. Lee, H.-S. Guan, C.-H. Wang, W.-N. Huang, S.-C. Tjong, C.-J. Chen, and W.-g. Wu, J. Biol. Chem. **280**, 9567(2005).

CONTACT E-MAIL
cjchen@nsrrc.org.tw